ELSEVIER

Journal of Magnetism and Magnetic Materials 191 (1999) 313–322

Journal of magnetism and magnetic materials

Torsion oscillation magnetometry (TOM) of Fe films on Ni(1 1 1)/W(1 1 0) substrates

H. Höche[a,*], H.-J. Elmers[b]

[a]*Max-Planck-Institut für Mikrostrukturphysik, Weinberg 2, D-06120 Halle (Saale), Germany*
[b]*Johannes Gutenberg-Universität Mainz, Staudingerweg 7, D-55099 Mainz, Germany*

Received 22 July 1998; received in revised form 23 September 1998

Abstract

Fe films 2–20 atomic monolayers (ML) thick have been deposited on Ni(1 1 1) films (4–60 ML) prepared on W(1 1 0) under UHV conditions. The Ni(1 1 1) films grow in a Nishijama–Wassermann orientation with a 3.6% lattice expansion along Ni[$\bar{2}$ 1 1] (‖ W[$\bar{1}$ 1 0]). On top of these slightly distorted Ni films iron is observed to grow preferentially in two mirror orientations. The saturation magnetization of these Fe films and the anisotropies of Fe/Ni bilayers have been studied using torsion oscillation magnetometry. The magnetization of the Fe films of 2.13 μ_B per atom is close to the bulk value of Fe. The out-of-plane surface (interface) anisotropy constant $K_s^{FeNi} = (-0.65 \pm 0.15)\,mJ/m^2$ of the bilayers prefers a magnetization perpendicular to the surface. The exceptionally high value of the volume anisotropy constant of the Fe films, $K_v^{Fe} = (+0.71 \pm 0.10)\,MJ/m^3 = (52.2 \pm 7.5)\,\mu eV/atom$, was ascribed to magnetoelastic contributions.

PACS: 75.70; 75.30.G; 75.50.B

Keywords: Ferromagnetic thin films; Bilayers; Magnetic anisotropy; Magnetic moment

1. Introduction

During the last decade much attention has been paid to the influence of the crystallographic structure of magnetic thin films on their magnetic properties [1]. Especially the behavior of FCC Fe films stabilized over a few atomic layers on single crystalline FCC substrates has attracted much experimental [2–14] and theoretical [15–19] interest. While bulk-like FCC Fe, only formed at high temperatures $T > 1183\,K$ or precipitated in a Cu matrix ($a_{FCC\,Fe} = 3.59$ Å), does not show any ferromagnetic behavior, distinct ferromagnetic states have been observed in epitaxial FCC Fe films. Theoretical calculations for FCC Fe crystals predict a non-magnetic state for small lattice constants (<3.61 Å) switching to a ferromagnetic state with a high moment of 2.6 μ_B (high-spin state) for larger lattice constants (>3.62 Å) [16]. Therefore, it is a challenge to imprint or even to trigger the structure of thin Fe films using appropriate substrates and thus to modify their magnetic properties.

*Corresponding author. Fax: +49-345-5511223; e-mail: hoeche@mpi-halle.de.

0304-8853/99/$ – see front matter
PII: S0304-8853(98)00380-1

The isotropic FCC lattice considered in theory cannot be realized in epitaxial films where the cubic lattice structure generally shows a distortion. Of special interest have been Fe films on Cu substrates ($a_{Cu} = 3.615$ Å) because of the particularly small lattice mismatch. On Cu(1 0 0), FCC Fe films (less than 4 ML thick) exhibit a high-spin phase [4,7], whereas those deposited on Cu(1 1 1) show a low spin state (0.6 μ_B) [2,14]. The dependence of the magnetic Fe moment on the lattice constant has been impressively demonstrated for thin (<3 ML) FCC Fe(1 1 1) films grown on (1 1 1) surfaces of CuAu alloys [3]. With the substrate lattice parameter increasing by changing the Au concentration of the alloy, there was a distinct rise of the mean Fe moment from about 0.6–2.6 μ_B. Recently, a similarly high spin state was deduced from Kerr measurements for FCC films prepared on a pure Cu(1 1 1) surface by pulsed laser deposition [14].

It is generally believed that a compression of the FCC Fe lattice results in a switch to the antiferromagnetic or non-magnetic state, see, e.g., Ref. [16]. Therefore, the application of Ni as a substrate for epitaxial Fe films is of special interest. Unlike copper, Ni exhibits two important features: (i) Ni is distinguished by the smallest lattice parameter of all FCC metals ($a_{Ni} = 3.524$ Å), i.e., about 2.5% smaller than that of Cu, and could therefore be expected to stabilize thin FCC Fe films with a very small atomic volume (the lattice parameter of FCC Fe at room temperature (RT) was predicted [17] to be 3.55 … 3.58 Å). (ii) Contrary to copper, Ni substrates are ferromagnetic, i.e., there occur polarization and coupling effects between the constituents of the Fe/Ni bilayer. In polycrystalline (<32 Å)Fe/(70 Å)Ni bilayers grown on Si(1 0 0) an FCC-like structure of Fe films was deduced even up to a thickness of about 32 Å of the Fe overlayer [11]. Moreover, what is of even more interest, these Fe films show an averaged magnetic Fe moment of $\mu_{Fe} = (0.2 \pm 0.2)\,\mu_B$. Therefore, these Fe films are assumed to be either antiferromagnetically ordered, or to exhibit almost vanishing Fe moments in agreement with the theoretical prediction. In contrast to that, for Fe films on Ni(1 1 1)/W(1 1 0) Sander et al. [12] proved a Kerr signal increasing with the Fe thickness.

In the present study, both the magnetic moment and the anisotropy of Fe/Ni bilayers have been studied by torsion oscillation magnetometry (TOM).

2. Experimental

The samples have been prepared and characterized in situ in a UHV torsion oscillation magnetometer [20]. The base pressure was less than 6×10^{-11} Torr. The UHV chamber was supplied with a combined low energy electron diffraction (LEED)/Auger electron spectroscopy (AES) system to characterize both the substrate surface and the growth of thin films on top of it. BeO crucibles were used for the thermal sublimation of Ni and Fe. The applied deposition rates (about 0.6 ML/min for Ni and 0.7 ML/min for Fe) and the total amount of the deposited metals have been measured by a quartz monitor mounted close to the substrate crystal.

In the present paper, the thicknesses of the films are given for Ni in bulk ML of FCC Ni(1 1 1) for Ni, and in bulk ML of BCC Fe(1 1 0) for Fe, irrespective of the structure of the deposited films. (The corresponding bulk lattice plane distances perpendicular to the surface are $d_{Ni} = 2.035$ Å and $d_{Fe} = 2.027$ Å at RT.) The deposited film thickness as determined by AES was found to vary by less than 5% over the whole sample. During the deposition of both Ni and Fe the overall pressure within the magnetometer did not exceed 2×10^{-10} Torr. On top of the W(1 1 0) substrate crystal Fe/Ni bilayers have been prepared in an area of $A = (30.0 \pm 0.7)$ mm^2 ($= 10.17$ mm $\times$ 2.95 mm). Prior to deposition the 0.18 mm thick rectangular W crystal (length parallel to the torsion axis: 15.0 mm, width: 2.95 mm) was cleaned by standard procedures [21] (heating in oxygen (10 min at 5×10^{-8} Torr) followed by flashing at temperatures as high as about 2000 K) to reduce the carbon contamination below the detection limit of our Auger system. Onto the freshly cleaned W(1 1 0) substrate a Ni film (usually 21 ML thick) was evaporated at RT and then magnetically characterized by TOM. Thereafter, a Fe film of a desired thickness (2–20 ML) was deposited at RT on top of the Ni film. Each experiment was concluded by a TOM measurement of the bilayer.

3. Structure of the films

The structures of the deposited films have been analyzed by LEED. In agreement with previous investigations on Ni/W(1 1 0) [12,21,22] a pseudomorphic growth of Ni has been observed up to about 0.4 ML. Thicker Ni films are known to grow in a Nishiyama–Wassermann (NW) orientation (Ni[0 $\bar{1}$ 1]‖W[0 0 1] and Ni[$\bar{2}$ 1 1]‖W[$\bar{1}$ 1 0]). A result typical of Ni films thicker than 3 ML is shown in Fig. 1, where the LEED spots of a W(1 1 0) surface are directly compared with those of a 6.0 ML Ni film. For this comparison, a surface region half-shadowed during the Ni deposition was analyzed. The sharp innermost LEED spots belong to the BCC W(1 1 0) surface, and the outer, slightly broadened ones, to the FCC Ni(1 1 1) film. The coincidence of the W and Ni spots along the W[$\bar{1}$ 1 0]‖Ni[$\bar{2}$ 1 1] direction indicates a 3.6% expansion of the separation distance of Ni atoms along Ni[$\bar{2}$ 1 1], whereas along [0 $\bar{1}$ 1] the bulk separation distance appears. The NW-orientation of thicker Ni(1 1 1) films with a 3.6% expansion along [$\bar{2}$ 1 1] reduces the sixfold symmetry of the Ni(1 1 1) surface of a bulk crystal. The expansion could be observed for films up to 8 ML in thickness. For thicker Ni films the LEED spots become rather broad indicating a rough morphology of the surface and preventing an accurate determination of the lattice structure. Although not experimentally observed the lattice expansion of the Ni film is assumed to persist for thicker films similar to Co on W(1 1 0) [24].

Fig. 2a shows a typical LEED pattern, which compares the structure of a Ni sublayer (6.0 ML) with that of a subsequently deposited Fe film (4.0 ML). Again, similarly to Fig. 1, a half-shadowed surface region is considered. As shown in the magnified parts, the spots are split into two or three more or less distinct spots. Fig. 2b presents a schematic view of the *k*-space around the (0 0) beam, which was achieved by image processing of Fig. 2a. The appearance of split spots shows that the Fe film does not grow in the pseudomorphic FCC(1 1 1) orientation.

Evaluating the LEED pattern in more detail allowed a model to be proposed in which the satellites occurring adjacent to the Ni spots are attributed to two twisted equivalent Fe unit surface cells (structural domains) simultaneously appearing in mirror orientations with respect to Ni[$\bar{2}$ 1 1] or Ni[0 $\bar{1}$ 1], respectively. In Fig. 2b, open and full circles are used to distinguish the LEED spots of the two different structural Fe domains. In Fig. 2c, the resulting real space surface lattice parameters of both structures are presented and compared with the experimentally determined NW Ni(1 1 1) surface mesh.

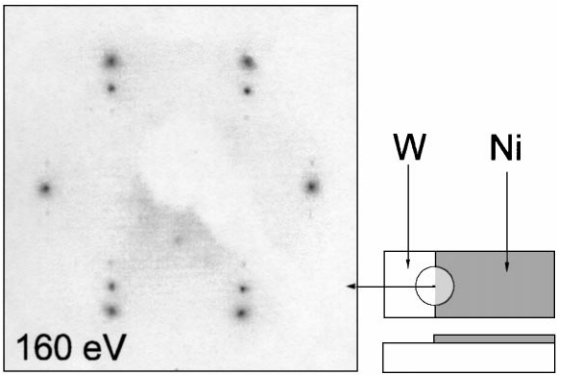

Fig. 1. LEED pattern of a W(1 1 0) surface region half-covered with 6.0 ML Ni.

The orientations of the different Fe domains with respect to the Ni substrate film are shown more clearly in the structure model given in Fig. 3. The domains are twisted against the Ni[0 $\bar{1}$ 1] direction by about $\pm 2.5^\circ$. It should be noted here that the satellite spots caused by the Fe film can only be observed up to about 8 ML, because the LEED patterns of thicker Fe films become more and more blurred. This indicates a 3D growth, which is supported by the observed two somewhat differently oriented Fe domains.

To decide whether the derived Fe unit surface mesh exhibits more similarities to an FCC-like structure than to a BCC-like one, in Fig. 4, it is compared with unit cells of both FCC Fe(1 1 1) [17] and BCC Fe(1 1 0). It is interesting that the deduced Fe surface unit mesh fits neither FCC Fe(1 1 1) nor BCC Fe(1 1 0). The angle of 123.2° enclosed by the surface unit vectors is close to the 120° of the FCC surface mesh (BCC surface structures distinguishing themselves by an angle of

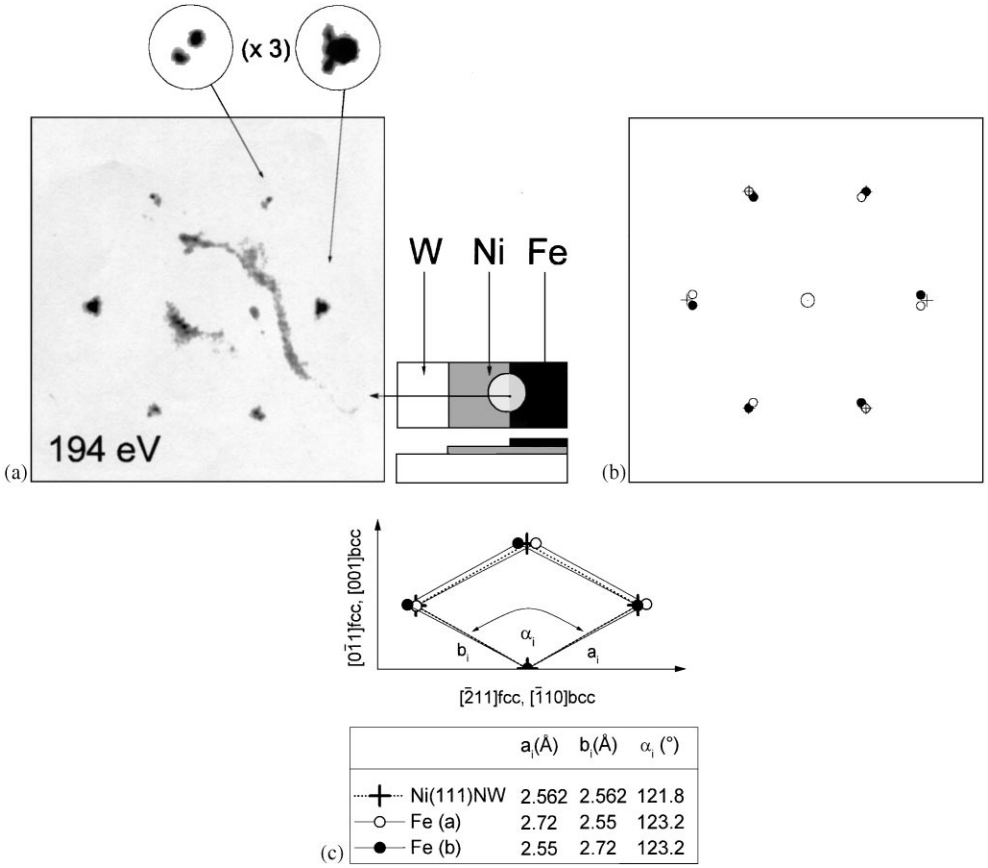

Fig. 2. (a) LEED pattern of a 6.0 ML Ni(1 1 1) film half covered with 4.0 ML Fe. The satellite peaks are due to the Fe deposition, (b) schematic view of the *k*-space, and (c) comparison of the surface unit vectors of the Ni(1 1 1) surface mesh (NW orientation, 3.6% expansion in [$\bar{2}$ 1 1] direction) with the deduced two Fe unit meshes showing mirror symmetry.

109.5°). However, the size of the observed Fe surface unit mesh (5.80 Å^2) is larger than that of the FCC structure (5.50 Å^2 with $a_{0,\mathrm{FCC}} = (3.565 \pm 0.015)$ Å [17]), but corresponds well to that of the BCC surface mesh (5.81 Å^2 with $a_{0,\mathrm{BCC}} = 2.866$ Å).

According to the elasticity theory changes to the in-plane spacing should result in changes to the interlayer separation distance. Experimentally, it was not possible to determine this interlayer spacing and thus to decide whether the Fe films on Ni(1 1 1) sublayers tend to an FCC- or a BCC-like structure. It should be mentioned, however, that, as shown by Sander et al. [12] using angle-resolved Auger spectroscopy, similarly prepared 3 ML Fe films grow in an FCC-like structure on top of Ni/W(1 1 0) substrates.

4. Torsion oscillation magnetometry

To characterize the magnetic properties of thin Fe/Ni bilayers torsion oscillation magnetometry (TOM) was performed at RT. The main features of TOM have been described previously in detail [20,25]. Therefore, solely some basics and the main components of the applied magnetometer are briefly mentioned here. In TOM experiments, small amplitude oscillations of the sample suspended on

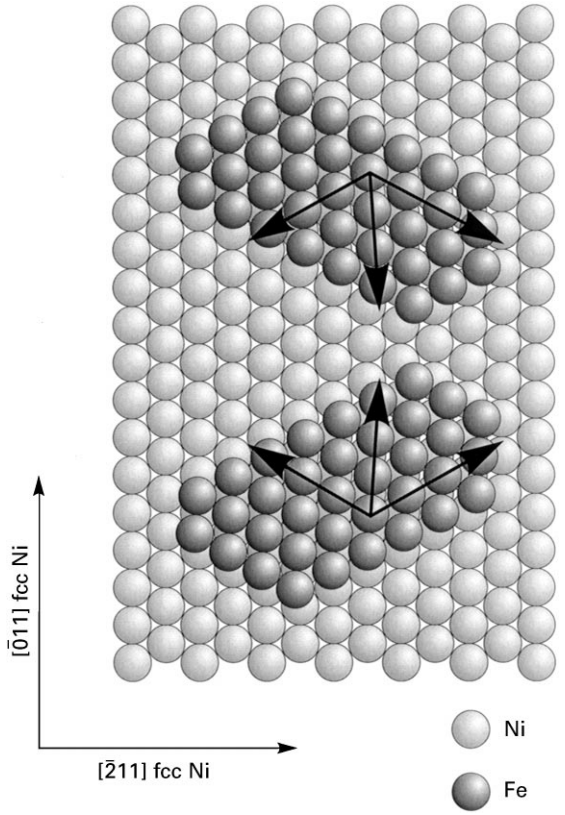

Fig. 3. Real-space representation of both the Ni(1 1 1) substrate film and the two structural Fe domains showing mirror planes of symmetry along Ni[0 $\bar{1}$ 1] and Ni[$\bar{2}$ 1 1].

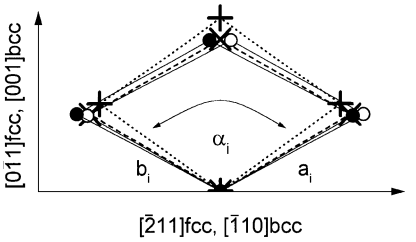

	a_i(Å)	b_i(Å)	α_i (°)
Fe (a)	2.72	2.55	123.2
Fe (b)	2.55	2.72	123.2
bcc Fe(110)	2.482	2.482	109.4
fcc Fe(111)	2.52	2.52	120.0

Fig. 4. Comparison of the experimentally observed Fe surface unit vectors with corresponding ones of a BCC(1 1 0) and an FCC(1 1 1) surface mesh.

a thin torsion filament are studied to determine the magnetic torque constant R as a function of the strength of a homogeneous external magnetic field H (in the present setup: $-0.3\ \mathrm{T} < \mu_0 H < +0.3\ \mathrm{T}$) applied perpendicular to the torsion axis (for details see, e.g., Refs. [20,25]). Both the Ni films [22] and the Fe (>1 ML)/Ni bilayers [12] on W(1 1 0) are known to be magnetized in-plane. Moreover, the easy axis of the magnetization of Ni(1 1 1)/W(1 1 0) was found [23] to be parallel to W[0 0 1]. In the present TOM investigations, a W(1 1 0) crystal was used with its [0 0 1] direction (in equilibrium) parallel to the external field.

The following consideration presupposes that the sample is homogeneously magnetized, with the magnetization vector deviating from the direction of the external field by only small angles. In our case, single-domain states can be expected for samples with an in-plane easy axis and an external field applied along the easy axis. The assumption of homogeneity along the film normal is justified because the film thicknesses considered here are much smaller than the exchange lengths.

For a given external magnetic field H, the magnetic torque constant

$$R = 4\pi^2 \Theta (1/T_H^2 - 1/T_0^2) \quad (1)$$

is obtained by measuring the oscillation periods T_0 without the applied field H and T_H with it. The moment of inertia Θ of the pendulum (substrate crystal including the sample holder) was experimentally determined to be $(62.5 \pm 2.5) \times 10^{-9}$ kg m^2 at RT [20]. During the torsional oscillations of the magnetic sample the external magnetic field provokes in a rotation of the magnetization vector, which, in turn, is coupled with the magnetic layer via the magnetic anisotropy. The effective anisotropy energy F of the deposited film, oscillating around its equilibrium position under the influence of an external field, is described in the quadratic approximation by

$$F(\vartheta)/V = L \cos^2 \vartheta, \quad (2)$$

with the effective anisotropy constant L. In this equation, V is the volume of the magnetic layer

(i.e., $V = At$, with A being the area, and t the thickness of the film) and ϑ is the angle between the film normal and the direction of the polarization J_s of the saturated film. In the above notation, positive values of L describe an in-plane magnetic easy axis.

Following Néel's approach [26], the effective anisotropy constant L of a thin magnetic film

$$L = [J_s^2/(2\mu_0) + K_v] + (1/t)K_s \quad (3)$$

can be subdivided into a volume term, which includes the shape anisotropy constant $J_s^2/(2\mu_0)$ and an additional volume anisotropy constant K_v, and a surface term being proportional to the sum K_s of all surface (interface) anisotropy constants and to the reciprocal of the film thickness t; $\mu_0 = 4\pi \times 10^{-7}$ H m^{-1}. Introducing the anisotropy field

$$H_{anis} = 2L/J_s\,(= F_{\vartheta\vartheta}(\vartheta = \pi/2)/m_s), \quad (4)$$

Eq. (1) can be expressed [25] by

$$R/H = m_s/(1 + (H/H_{anis})), \quad (5)$$

$m_s\,(= J_s V)$ denotes the magnetic moment (in saturation) of the sample and $F_{\vartheta\vartheta}(\pi/2)$ is the second derivative of the magnetic free energy in the equilibrium position.

The above hyperbolic function, Eq. (5), which describes the dependence of the magnetic torque constant $R(H)$ on the applied external field H, was fitted to the experimental $R(H)$ curves. Such a fit yields both the magnetic moment m_s and the effective anisotropy field H_{anis} of a thin magnetic film.

5. Magnetic results

A typical result of our TOM experiments is shown in Fig. 5. Immediately after the Ni deposition (here 20.6 ML) we determined the magnetic torque constant $R(H)$ for several fields. To simplify matters we plotted R/H as a function of H, with R/H being a rough measure of the magnetic moment of the sample (see Eq. (5)). The magnetic moment $m_s^{Ni}\,(= J_s^{Ni} V^{Ni})$ and the anisotropy field H_{anis}^{Ni} resulting from a least squares fit are given in the figure. Then, on top of the Ni film we deposited a Fe film of nearly the same thickness (20.5 ML), and finally measured again using TOM, see the upper curve in Fig. 5. The evaluation resulted in values of m_s^{FeNi} and H_{anis}^{FeNi} for the present Fe(20.5 ML)/Ni(20.6 ML) bilayer. The increase of the magnetic moment $\Delta m_s = m_s^{FeNi} - m_s^{Ni}$ related to the magnetic moment of the Fe film is roughly three times larger than the moment of the Ni film.

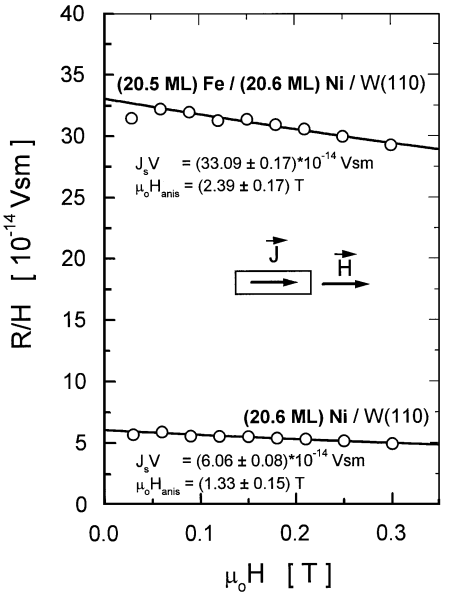

Fig. 5. R/H curves of a 20.6 ML Ni(1 1 1) film before and after the deposition of 20.5 ML Fe.

For a systematic investigation of the magnetic properties of the Fe film we prepared a series of samples of a constant Ni film thickness of 21 ML, but with varying Fe film thickness. Additional samples with thinner and thicker Ni films were prepared in order to check the independence of the Fe film properties from the Ni substrate thickness.

For all samples, Fig. 6 summarizes the changes of the magnetic moment $\Delta m_s = m_s^{FeNi} - m_s^{Ni}$ as a function of the thickness $D_{Fe} = t_{Fe}/d_{Fe}$ of the deposited Fe films. Starting with the thinnest Fe film (2 ML) there was a linear increase of Δm_s with film thickness D_{Fe}. A linear least squares fit was performed for the data from the series with a constant Ni film thickness of 21.0 ML resulting in a slope $S^{Fe} = \Delta m_s/D_{Fe} = 1284.5 \times 10^{-17}$ Vsm and a vertical axis section $\Delta m_{so} = 351.3 \times 10^{-17}$ Vsm. From the slope $S^{Fe} = J_s^{Fe} A d_{Fe} = \mu_{Fe} A/n_{Fe}$, the bulk magnetization

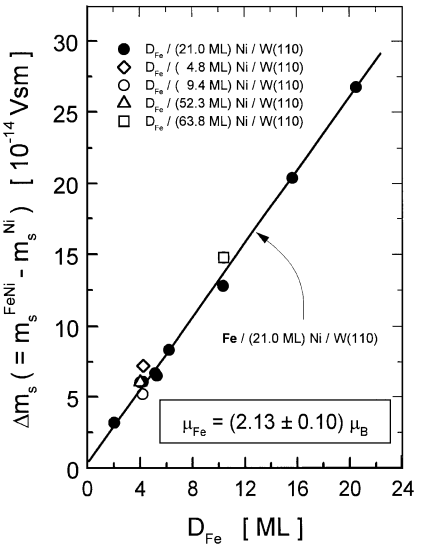

Fig. 6. Increase of the magnetic moment Δm_s of Ni(1 1 1) films due to the Fe deposition. As indicated some of the Fe films were prepared on Ni(1 1 1) substrate films of different thicknesses. Note that the straight line was determined by the linear regression of the data obtained for Fe films all grown on top of (21 ML) Ni sublayers.

J_s^{Fe} or the bulk atomic moment μ_{Fe} of the Fe film could be directly determined, where $n_{Ni} = 18.598$ atoms/nm^2 and $n_{Fe} = 17.215$ atoms/nm^2 are the two-dimensional densities of atoms in one atomic layer within FCC Ni and BCC Fe films. The error of R/H (see Eqs. (1) and (5)) resulting from the determination of the absolute values of film thickness D_{Fe}, the area A of the deposited Fe film and the moment of inertia Θ is relatively large. Therefore we prefer to determine primarily the ratio $\mu^{Fe}/\mu^{Ni} = (S^{Fe}/S^{Ni})(n_{Ni}/n_{Fe})$, which is independent of these experimental parameters. In addition, a previous TOM investigation (carried out in preparation of the present study) has been used, where the increase of the magnetic moment of the W(1 1 0) substrate with increasing Ni film thickness was determined, yielding $S^{Ni} = 372.2 \times 10^{-17}$ Vsm/ML. Finally, assuming the Ni bulk value $\mu_{Ni} = 0.57\ \mu_B$ [28] as a good approach to the Ni atoms within the substrate layer the magnetic moment of the Fe atoms is found to be

$$\mu_{Fe} = (2.13 \pm 0.10)\ \mu_B.$$

The anisotropy fields H_{anis}^{FeNi} have been evaluated to determine the bulk and surface anisotropy constants K_v^{Fe} and K_s^{FeNi}. To this end the change of the anisotropy field of (21 ML)Ni(1 1 1) films due to Fe deposition was studied as a function of the Fe coverage D_{Fe}. Corresponding to Eqs. (2) and (3) the anisotropy energy of an Fe/Ni bilayer on W(1 1 0) is given by

$$F^{FeNiW}(\vartheta)/A = \{[(J_s^{Fe})^2/(2\mu_0) + K_v^{Fe}]t_{Fe} + [(J_s^{Ni})^2/(2\mu_0) + K_v^{Ni}]t_{Ni} + K_s^{FeNi}\}\cos^2\vartheta, \quad (6)$$

where the first two terms describe the volume anisotropy contributions of both the Fe film and the Ni film. The shape anisotropy terms $(J_s^{Fe})^2/(2\mu_0)$ and $(J_s^{Ni})^2/(2\mu_0)$ consider Fe and Ni films with a homogeneous bulk magnetization. Small deviations caused by modified magnetization values at the interfaces are neglected. The interface anisotropy constant K_s^{FeNi} summarizes the contributions of all interfaces (UHV/Fe, Fe/Ni, and Ni/W) of the bilayer.

For a straightforward evaluation of the experimental results it is of advantage to consider the second derivative of the magnetic free energy in the equilibrium position of the saturated magnetic film ($\vartheta = \pi/2$, i.e., parallel to the external magnetic field). The second derivative is given (see Eq. (4)) by

$$F_{\vartheta\vartheta}^{FeNi}/A|_{\vartheta=\pi/2} = (m_s^{FeNi}/A)H_{anis}^{FeNi} = [(J_s^{Fe})^2/\mu_0 + 2K_v^{Fe}]t_{Fe} + [(J_s^{Ni})^2/\mu_0 + 2K_v^{Ni}]t_{Ni} + 2K_s^{FeNi}. \quad (7)$$

From the data of Ni films without Fe coverage the volume anisotropy term, $(J_s^{Ni})^2/2\mu_0 + K_v^{Ni} = (0.10 \pm 0.01)$ MJ/m^3, was determined in preparation for the present investigation. Using this value both the desired quantities K_v^{Fe} and K_s^{FeNi} can be ascertained. To do this, $F_{\vartheta\vartheta}^{FeNi}/A$ (see Eq. (7)) is reduced by the volume anisotropy term of the Ni substrate layer,

$$\begin{aligned} F_{\vartheta\vartheta}^{FeNi}/A|_{\vartheta=\pi/2} - 2[(J_s^{Ni})^2/(2\mu_0) + K_v^{Ni}]t_{Ni} &= m_s^{FeNi}H_{anis}^{FeNi}/A \\ &\quad - 2[(J_s^{Ni})^2/(2\mu_0) + K_v^{Ni})]t_{Ni} \\ &= 2[(J_s^{Fe})^2/(2\mu_0) + K_v^{Fe}]t_{Fe} + 2K_s^{FeNi} \end{aligned} \quad (8)$$

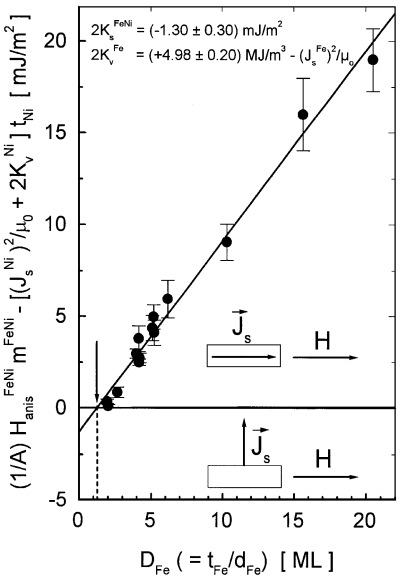

Fig. 7. Determination of the anisotropy constants K_v^{Fe} and K_s^{FeNi} from the dependence of $(1/A)F_{gg}^{FeNi}(\pi/2) - 2[(J_s^{Ni})^2/(2\mu_0) + K_v^{Ni})]t_{Ni}$ of a Fe/(21 ML)Ni bilayer on the deposited Fe film thickness, see Eqs. (7) and (8).

and plotted as a function of the thickness D_{Fe} of the deposited Fe films, see Fig. 7. As predicted by Eq. (8) there is a linear increase with the Fe thickness. A linear least-squares fit results in $K_v^{Fe} = (0.71 \pm 0.10)$ MJ/m^3, i.e., about (-52.2 ± 7.5) μeV/atom, for the volume anisotropy constant and in $K_s^{FeNi} = (-0.65 \pm 0.15)$ mJ/m^2 , respectively, for the interface anisotropy constant. This evaluation regards a shape anisotropy constant of $(J_s^{Fe})^2/(2\mu_0) = 1.78$ MJ/m^3 directly obtained from the atomic Fe moment determined above.

6. Discussion

The magnetic moment of the bilayer samples determined by TOM linearly increases with their Fe film thickness. The absolute value of the atomic Fe moment is close to the RT bulk value of μ_{Fe}(bulk) = 2.17 μ_B [28]. Thus, in the present study of Fe/Ni bilayers on W(1 1 0) there is no indication of a lowered magnetic moment expected to appear in thin Fe films of a reduced atomic volume as observed in Ref. [11] for polycrystalline Fe(< 30 Å)/Ni(70 Å) bilayers on Si(1 0 0). The atomic Fe volume could not be determined by our structural LEED investigations of Fe films on top of Ni(1 1 1) substrate films since we had no experimental means to study the interlayer distance of the Fe films.

We assume that the behavior of our Fe/Ni films on W(1 1 0) compared to that of the bilayers on Si(1 0 0) is due to the missing sixfold symmetry of the Ni film and the resulting simultaneous growth of Fe in two distorted structural domains. The increase of the total magnetic moment of our samples (see Fig. 6) shows only a small value of the Δm_s-intercept, viz. $\Delta m_{so}(D_{Fe} = 0)$ $(= 351 \times 10^{-17}$ Vsm). This indicates a compensation or negligible influences of both the size effect (due to the finite temperature of the measurement) and the interface effect (caused by the symmetry breaking at the interfaces and by the polarization effects at the Ni/Fe interface) [27].

The surprisingly high value $K_v^{Fe} = (0.71 \pm 0.10)$ MJ/m^3 of the volume anisotropy constant, which is much larger than the crystalline anisotropy 0.046 MJ/m^3 [28], is presumably due to mainly magnetoelastic contributions. Considering the BCC bulk magnetostriction constants of iron [28] as a rough approximation, one would need a homogeneous strain of the order of 10% to explain the experimental data, not uncommon for epitaxial films being only a few atomic monolayers thick. The large volume anisotropy term in Fe films thicker than 15 ML, however, is unusual and cannot be explained easily. This surprising behavior is probably associated with magnetoelastic contributions arising from the growth process of the Fe films, which right from the beginning grow in two equivalent but somewhat twisted structural domains on top of the slightly distorted Ni sublayer.

The negative effective surface (interface) anisotropy constant of the bilayers, $K_s^{FeNi} = (-0.65 \pm 0.15)$ mJ/m^2, implies that the surface (interface) anisotropy prefers a magnetization perpendicular to the surface. Due to the competition between volume and surface anisotropies perpendicular magnetization can only be expected to occur for Fe thicknesses lower than 1.2 ML (see Fig. 7: point of intersection of both straight line and

horizontal axis). In fact, using the magneto-optical Kerr effect Sander et al. [13] found out that a cap layer of only 1 ML Fe induces a spin reorientation of a Ni(<10 ML) film on W(1 1 0) from in-plane to perpendicular to the film. We observed the same behavior in corresponding TOM experiments, not reported here. In our experiments, however, the perpendicular magnetization of 10 ML Ni/W(1 1 0) due to one added ML Fe was observed to be unstable against a residual gas exposure. At a coverage of about 0.5 Langmuir the easy axis changes from perpendicular to in-plane.

7. Summary

In the present paper the magnetic properties of Fe films (>2 ML) grown on bulk like Ni(1 1 1) films deposited on W(1 1 0) have been studied by UHV torsion oscillation magnetometry. Due to the reduced symmetry of the slightly distorted Ni(1 1 1) films (NW orientation, +3.6% misfit along Ni[$\bar{2}$ 1 1]‖W[$\bar{1}$ 1 0]) the subsequently deposited Fe films do not grow pseudomorphically on the Ni(1 1 1) film but in two equivalent structural domains showing mirror planes of symmetry along Ni[$\bar{2}$ 1 1] and Ni[0 $\bar{1}$ 1]. It has not yet been possible to attribute unequivocally the surface unit cell of the deposited Fe films, deduced from LEED observations, to either an FCC-like structure or a BCC-like one.

From TOM experiments of Fe/Ni bilayers on W(1 1 0) the bulk atomic magnetic moment of Fe atoms $\mu_{Fe} = (2.13 \pm 0.10)\,\mu_B$ was evaluated, which is close to the RT bulk value of 2.17 μ_B.

The observed high value of the volume anisotropy of the Fe/Ni bilayers ($K_v^{Fe} = (0.71 \pm 0.10)\,MJ/m^3$) is most likely caused by local magnetoelastic contributions due to the complicated growth of Fe films, which is controlled by the simultaneous appearance of two small slightly twisted structural domains. The evaluation of the effective anisotropy fields of Fe/Ni bilayers as a function of the Fe film thickness has shown that the surface (interface) anisotropy $K_s^{FeNi} = (-0.65 \pm 0.15)\,mJ/m^2$ prefers a perpendicular magnetization. This result is confirmed by a previous magneto-optical Kerr effect study of Sander et al. [13], where thin Ni films (<15 ML) are observed to undergo a magnetization transition from in-plane to perpendicular due to the deposition of about 1 ML Fe.

Further studies, especially of the interlayer distance, will be necessary to elucidate the real nature of the Fe films (atomic Fe volume) grown on top of Ni(1 1 1) substrate films prepared on W(1 1 0).

Acknowledgements

The support by the Deutsche Forschungsgemeinschaft of the present work, as the result of a several months' working stay of H.H. at the University of Mainz, is gratefully acknowledged. The authors would like to thank Prof. U. Gradmann and Prof. J. Kirschner for careful reading the manuscript.

References

[1] U. Gradmann in: K.H.J. Buschow (Ed.), Handbook of Magnetic Materials, vol. 7, Elsevier, Amsterdam, 1993, and references therein.
[2] W. Kümmerle, U. Gradmann, Phys. Stat. Sol. (a) 45 (1978) 171.
[3] U. Gradmann, H.O. Isbert, J. Magn. Magn. Mater. 15–18 (1980) 1109.
[4] R.D. Ellerbrock, A. Fuest, A. Schatz, W. Keune, R.A. Brand, Phys. Rev. Lett. 61 (1988) 475.
[5] D. Li, M. Freitag, J. Pearson, Z.Q. Qiu, S.D. Bader, Phys. Rev. Lett. 72 (1994) 3112.
[6] J. Thomassen, F. May, B. Feldmann, M. Wuttig, H. Ibach, Phys. Rev. Lett. 69 (1994) 3112.
[7] M. Wuttig, B. Feldmann, T. Flores, Surf. Sci. 331–333 (1995) 659.
[8] J. Fassbender, U. May, B. Schirmer, R.M. Jungblut, B. Hillebrands, G. Güntherodt, Phys. Rev. Lett. 75 (1995) 4476.
[9] M. Straub, R. Vollmer, J. Kirschner, Phys. Rev. Lett. 77 (1996) 743.
[10] M. Zharnikov, A. Dittschar, W. Kuch, C.M. Schneider, J. Kirschner, J. Magn. Magn. Mater. 174 (1997) 40.
[11] Y. Li, C. Polaczyk, F. Klose, J. Kapoor, H. Maletta, D. Riegel, Phys. Rev. B 53 (1996) 5541.
[12] D. Sander, A. Enders, C. Schmidthals, J. Kirschner, H.L. Johnston, C.S. Arnold, D. Venus, J. Appl. Phys. 81 (1997) 4702.
[13] D. Sander, C. Schmidthals, A. Enders, J. Kirschner, Phys. Rev. B 57 (1998) 1406.

[14] J. Shen, P. Ohresser, Ch.V. Mohan, M. Klaua, J. Barthel, J. Kirschner, Phys. Rev. Lett. 80 (1998) 1980.
[15] O.K. Andersen, J. Madsen, U.K. Poulsen, O. Jepsen, J. Kollar, Physica B 86–88 (1977) 249.
[16] V.L. Moruzzi, P.M. Marcus, P.C. Pattnaik, Phys. Rev. B 37 (1988) 8003.
[17] K. Heinz, P. Bayer, S. Müller, J. Kübler, Phys. Rev. B 39 (1989) 6957.
[18] R. Lorenz, J. Hafner, Phys. Rev. B 54 (1996) 15937.
[19] T. Asada, S. Blügel, Phys. Rev. Lett. 79 (1997) 507.
[20] J. Kohlhepp, Ph.D. Thesis, TU Clausthal, Germany, 1995.
[21] J. Kolaczkiewicz, E. Bauer, Surf. Sci. 144 (1984) 495.
[22] M. Farle, A. Berghaus, Y. Li, K. Baberschke, Phys. Rev. B 42 (1990) 4873.
[23] Y. Li, K. Baberschke, Phys. Rev. Lett. 68 (1992) 1208.
[24] H. Fritzsche, J. Kohlhepp, U. Gradmann, Phys. Rev. B 51 (1995) 15933.
[25] U. Gradmann, W. Kümmerle, R. Tamm, Appl. Phys. 10 (1976) 219.
[26] L. Néel, J. Phys. Rad. 15 (1954) 225.
[27] K. Wagner, N. Weber, H.J. Elmers, U. Gradmann, J. Magn. Magn. Mater. 167 (1997) 21.
[28] Landolt-Börnstein, New Series, Vol. III/19a, Berlin, 1986.